

UNDULATOR-BASED LASER WAKEFIELD ACCELERATOR ELECTRON BEAM DIAGNOSTIC*

M.S. Bakeman[#], W. Leemans, K. Nakamura, K.E. Robinson, C.B. Schroeder, C. Toth, LBNL, Berkeley, CA 94720, U.S.A.

Abstract

The design and current status of experiments to couple the THUNDER undulator to the LOASIS Lawrence Berkeley National Laboratory (LBNL) laser wakefield accelerator (LWFA) are discussed. Currently the LWFA has achieved quasi-monoenergetic electron beams with energies up to 1 GeV [1]. These ultra-short, high-peak-current, electron beams may be well suited for driving a compact XUV free electron laser (FEL) [2], provided that the energy spread and emittance is sufficiently low for achieving a high brightness source. The electron beam energy spread and emittance can be measured with high precision by using an insertion device such as an undulator and observing changes in the spontaneous emission spectrum. The initial experiments will use spontaneous emission from 1.5 m of undulator. Later experiments will use up to 5 m of undulator with a goal of a high gain, XUV FEL.

INTRODUCTION

Recently laser wakefield acceleration (LWFA) up to a GeV has been realized at the LOASIS Laboratory at Lawrence Berkeley National Laboratory (LBNL) [1]. In these experiments, electron beams were characterized utilizing a 1.25 T round pole magnet spectrometer [3]. While the energy resolution of the spectrometer was sufficient for these initial experiments, electrons beams with energy spread as small as the resolution of the spectrometer have been observed. In order to quantify the energy spread with resolution on the order of 0.25%, and the emittance of the electron beam experiments are beginning to couple the THUNDER undulator [4] with the LOASIS LWFA.

Energy Spread and Emittance

The wavelength of the optical radiation emitted by a relativistic electron beam on-axis in a linearly polarized undulator is given by

$$\lambda = \frac{\lambda_u}{2\gamma^2} \left(1 + \frac{K^2}{2} \right) \quad (1)$$

where λ_u is the magnetic undulator period, γ is the electron beam energy in units of mc^2 , and K is the dimensionless wiggler parameter defined as

$$K = \frac{B_0 e \lambda_u}{m_0 c 2\pi} \quad (2)$$

where c is the speed of light and m_0 is the rest mass of the electron, B_0 is the maximum magnetic field of the undulator and e is the charge of the electron. For the THUNDER undulator at minimum gap, $K=1.85$. We can see from Eqn. (1) that the wavelength spread of the optical spectra is directly related to the electron beam energy spread. The optical spectra of the undulator radiation have been modeled numerically using the synchrotron radiation code SPECTRA [5], and examples of spectra are shown in Fig. 1 for a 500 MeV electron beam. These results show that the optical harmonic width is a good measure of the electron beam energy spread.

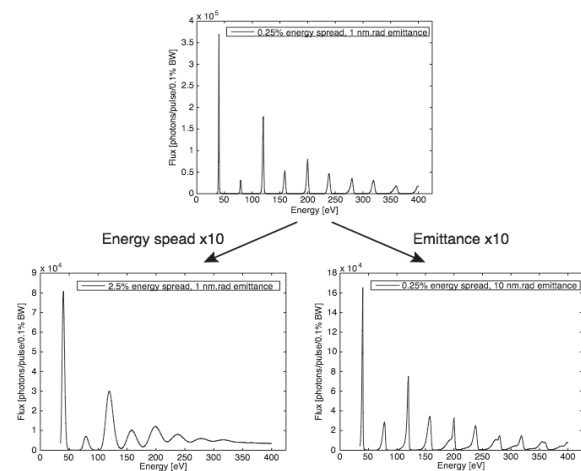


Figure 1: Numerical calculations showing the changes in the spontaneous emission optical spectra from the THUNDER undulator when varying the e-beam's energy spread and emittance by an order of magnitude. All values calculated for 66 magnetic periods of the THUNDER undulator with a 500 MeV beam.

Quantitatively the beam emittance can be measured by the on-axis flux ratio of the even optical harmonics to the odd optical harmonics (being ideally zero for a zero-emittance electron beam). Fig. 1 shows the changes in on-axis optical spectra emitted from the undulator, corresponding to an order of magnitude increase in energy spread (Fig. 1, bottom left) and emittance (Fig. 1, bottom right). Fig. 2 shows the expected spontaneous emission optical line width versus beam energy spread and the harmonic flux ratios (2nd to 1st harmonics and 2nd to 3rd harmonics) versus geometric emittance.

*Work supported by the Director, Office of Science, of the US Department of Energy under contract No. DE-AC02-05CH11231, and NSF Grant 0614001.

[#]msbakeman@lbl.gov

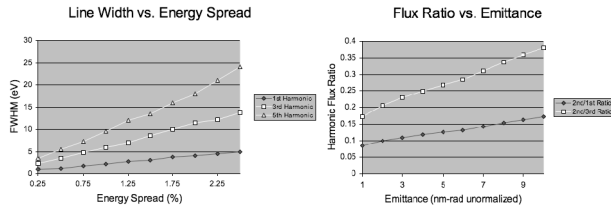


Figure 2: Left: Spontaneous emission optical harmonic line width as a function of the electron beam energy spread for the first three odd harmonics. Right: The flux ratio between the second and first harmonics and the second and third harmonics as a function of the beam emittance. All values were calculated for 66 magnetic periods with a 500 MeV electron beam.

THUNDER UNDULATOR

The Tapered Hybrid Undulator (THUNDER) [4] is a rare earth permanent magnet undulator, comprised of 10 sections of 0.5 m each, containing magnets made of SmCo₅ and vanadium permendur poles. Table 1 lists the operating parameters of the THUNDER undulator.

Table 1: THUNDER Undulator Specifications

THUNDER SPECIFICATIONS	Values
Length	5 m
Total Magnetic Period	2.18 cm
Number of Periods	220
Peak Field	1.02 T
Wiggler Parameter K	1.85
Betatron Period (500 MeV)	3.7 m
FEL Resonant Wavelength (500 MeV)	31 nm

The undulator sections have been magnetically tuned and characterized at LBNL using a Fanamation Coordinate Measuring Machine (CMM). The probe on the CMM has been fitted with a magnetic Hall probe, so that mechanical as well as magnetic measurements can be automated with micron resolution. The undulator sections are magnetically aligned using a mechanical separation structure with differential screws allowing for micron scale physical adjustments of the undulator sections.

Magnetic Tuning

In the coordinate frame where the electron is travelling in the s direction the equation of motion for the electron is given by

$$\frac{\partial^2 x}{\partial s^2} = \frac{e}{\gamma m_0 c} \left(B_y - \frac{\partial y}{\partial s} B_s \right) \quad (3)$$

The first integration of this equation yields the electron horizontal deflection angle from the s -axis, and the second integration yields the total electron horizontal deflection from the s -axis. Assuming a perfectly sinusoidal field without any errors the trajectory is given by

$$x(s) = \frac{B_0 e}{\gamma m_0 c} \left(\frac{\lambda_u}{2\pi} \right)^2 \sin \left(\frac{2\pi s}{\lambda_u} \right) \quad (4)$$

The optical phase error of the electron beam with respect to the optical radiation field is given by

$$\phi(s) = \frac{\pi}{\lambda_p \gamma^2} \int_{-\infty}^s \left[1 + \gamma^2 (\theta_x^2 + \theta_y^2) \right] ds \quad (5)$$

where λ_p is the wavelength of the optical radiation and θ_x and θ_y are the electron deflection angles from the s -axis. Both the horizontal deflection of the electron beam from the undulator axis as well as the optical phase error have been minimized during magnetic tuning in order to optimize the spontaneous radiation emission (Fig. 3).

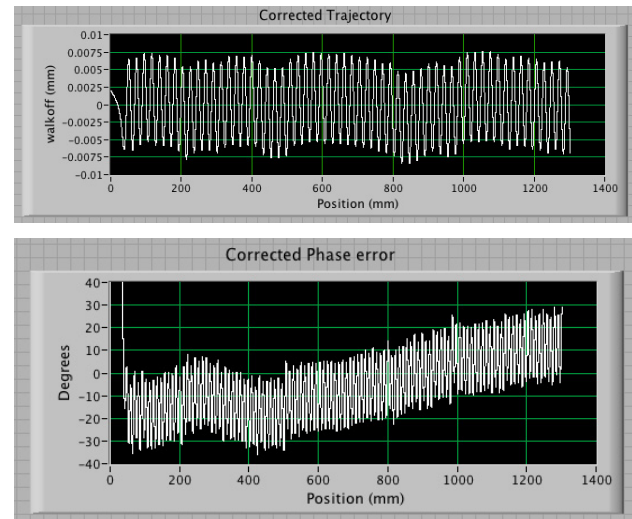


Figure 3: Magnetic data from 1.3 m of undulator after undergoing tuning, showing the electron horizontal deflection from the undulator axis and the optical phase error.

Magnetic tuning was accomplished through magnetic sorting and shimming. Course tuning was done by magnetic sorting where individual magnets that were producing large errors in the electron trajectory and optical phase are replaced by more suitable magnets. Fine

tuning was done by magnetic shimming where, 100 micron thick steel shims were cut by water jet and placed onto the magnets on both sides of a vanadium permendur pole. In this way the magnetic flux from each individual pole piece could be reduced in order to optimize the electron trajectory and optical phase error. As can be seen from Fig. 3 the maximum trajectory deviation from the undulator axis has been reduced to 8 microns and the maximum optical phase error has been reduced to 35 degrees.

With the magnetic tuning completed, gap blocks will now be machined to set the final magnetic gap distance, with final alignment being surveyed using the CMM touch probe. The final alignment of the undulator sections will be re-established and validated to micron precision in the LOASIS laboratory using a portable coordinate measuring machine.

OPTICAL SPECTRA WITH UNDULATOR FIELD ERRORS

Magnet sorting and shimming has significantly reduced the magnetic errors in the undulator. To assess the quality of the actual field and the impact of the errors on the photon flux from the undulator, numerical simulations of the undulator flux using the SPECTRA code [5] have been carried out using the magnetic field data measured with the Hall probe (Fig. 4).

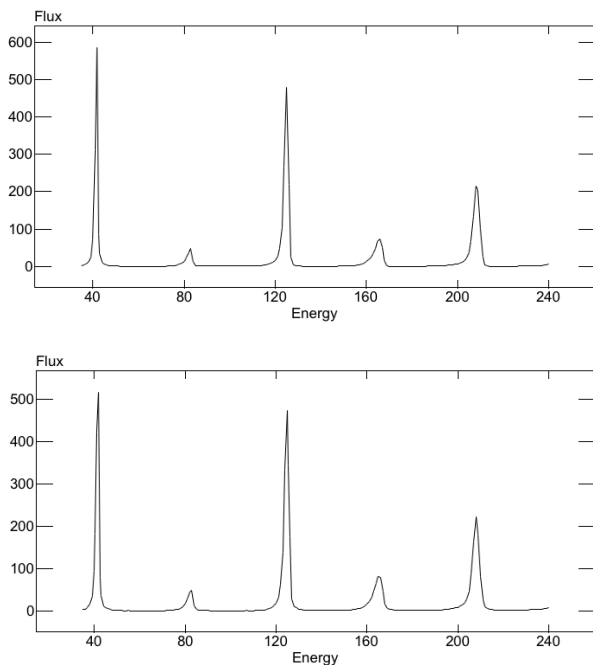


Figure 4: Photon flux (per 0.1% bandwidth) from a perfect undulator above and from the THUNDER undulator below. Both simulations were carried out using 500 MeV electrons with 10 pC of charge, an energy spread of 0.25% and a normalized transverse emittance of 1.0 mm-mrad.

From Fig. 4 it can be seen that relative to the other harmonics, the fundamental harmonic at 40 eV has been attenuated the most due to magnetic field errors. As evidence for near optimum tuning, the overall attenuation of the first harmonic is less than 16% of the flux at 0.1% of the bandwidth compared to a perfect undulator. Fluxes of this order are sufficient for our initial experiments. In addition a micro channel plate based spectrometer will be used to measure the spectra allowing improved signal to noise in our initial experiments.

SUMMARY

In summary, a conceptual design of an undulator-based electron beam diagnostic to be used in conjunction with the LOASIS LWFA 500 MeV electron beam has been presented. Details of the THUNDER undulator and its magnetic characterization and tuning have been provided. Initial experiments will use the observed changes in spontaneous emission from 1.5 m of undulator to measure the energy spread and the emittance of the electron beam. Later experiments will use up to 5 m of undulator with a goal of a compact, high gain, XUV FEL

ACKNOWLEDGMENTS

The contributions from the LBNL LOASIS staff and LBNL machine shops and discussions with F. Gruener of MPQ are gratefully acknowledged. We would like to express our appreciation to Boeing Phantom Works for making the THUNDER undulator available through an extended loan for these experiments, and for shipment of THUNDER to LBNL. This work was supported by the Director, Office of Science, of the US Department of Energy under contract No. DE-AC02-05CH11231, and NSF Grant 0614001.

REFERENCES

- [1] W.P. Leemans et al., *Nature Physics*, Volume 2, Issue 10, pp. 696-699 (2006).
- [2] C.B. Schroeder et al., *Proceedings of the Thirteenth Advanced Accelerator Concepts Workshop*, pp. 637 (2008).
- [3] K. Nakamura et al., *Review of Scientific Instruments*, Volume 79, pp. 53301 (2008).
- [4] K.E. Robinson et al., *IEEE Journal of Quantum Electronics*, Volume 23, Issue 9, pp. 1497- 1513 (1987).
- [5] T. Tanaka and H. Kitamura, *J. Synchrotron Radiation*, Volume 8, pp. 1221 (2001).